Journal of Hazardous Materials 205–206 (2012) 118–125

Contents lists available at SciVerse ScienceDirect

Journal of Hazardous Materials

journal homepage: www.elsevier.com/locate/jhazmat

Synthesis of 4-vinylpyridine–divinylbenzene copolymer adsorbents for microwave-assisted desorption of benzene

Qing Bo Meng[a], Go-Su Yang[b], Youn-Sik Lee[a,*]

[a] Division of Chemical Engineering, Nanomaterials Processing Research Center, Chonbuk National University, 567 Baekje-daero, Deokjin-gu, Jeonju-si, Jeollabuk-do 561-756, Republic of Korea

[b] Department of Environmental Engineering, Chonbuk National University, 567 Baekje-daero, Deokjin-gu, Jeonju-si, Jeollabuk-do 561-756, Republic of Korea

ARTICLE INFO

Article history:
Received 7 October 2011
Received in revised form
14 December 2011
Accepted 15 December 2011
Available online 23 December 2011

Keywords:
Polymer adsorbent
4-Vinylpyridine
Adsorption
Nonpolar VOCs
Microwave-assisted desorption

ABSTRACT

Reports on the development of polymer adsorbents for microwave-assisted desorption of nonpolar volatile organic compounds (VOCs) are rare. In this study, we synthesized macroporous polymeric adsorbents with hydrophilic methyl pyridinium units for microwave-assisted desorption of nonpolar VOCs. The benzene adsorption and desorption properties of the adsorbents were investigated under both dry and humid conditions. Under humid conditions, as the content of the hydrophilic methyl pyridinium units in the adsorbents increased from 0 to 20%, the adsorption capacity of benzene decreased from about 21 to 7 mg/g, while the desorption efficiency of benzene increased significantly from 48 to 87%. The maximum concentration of desorbate also increased significantly as the content of the hydrophilic units was increased under humid conditions. We attributed the enhanced desorption efficiency mainly to more adsorbed moisture, which indirectly allowed heating of the polymer adsorbents to higher temperatures upon irradiation with 600 W microwaves.

© 2011 Elsevier B.V. All rights reserved.

1. Introduction

Existing methods for removing volatile organic compounds (VOCs), which are produced in many industrial processes, include absorption, adsorption, condensation, and incineration. Compared with other separation techniques, adsorption is the most efficient and economical method to remove low to moderate concentrations of VOCs, especially when recovery of the desorbed VOCs is also required [1]. Two conventional methods are used to regenerate adsorbents: steam and hot gas. In either case, the hot fluid not only heats the adsorbents, but also purges the adsorbates from the adsorbents [2]. However, these methods dilute the exhausted VOCs significantly and consequently increase the cost of cooling the entire exhausted gas down to the condensation temperatures of VOCs [3].

In contrast, dielectric heating by microwaves is a very effective and economical method to recover adsorbed VOCs, because microwaves can irradiate adsorbed VOCs directly and heat can be produced internally within the material instead of the requirement for an external heat source [2]. Dielectric heating by microwaves has the advantages of better control of desorption, a higher desorbate concentration, less purge gas consumption, and a lower process temperature [4]. Because of these advantages, the microwave-based regeneration method has attracted great interest [5–8].

Adsorbents are a critical component of a VOC recovery system. Adsorbents should have sufficient adsorption capacity as well as physical, chemical, and thermal stability [9]. Various adsorbents have therefore been studied extensively. For example, activated carbons are commonly used in many adsorption processes because of their high adsorption capacity and ready availability [10,11]. However, activated carbons have some drawbacks such as pore clogging, hygroscopicity, and a lack of regenerative ability. Moreover, activated carbons are flammable. Zeolite adsorbents can be used as alternatives to activated carbons [12,13], but their high cost limits their application [14]. In addition, regeneration of zeolites usually requires even higher temperatures than activated carbons [15].

Macroporous polymer beads are highly crosslinked networks with high porosity, and are widely used as ion exchange resins, chromatography column packing materials, catalyst supporters, and adsorbents. In general, they are prepared by suspension polymerization of divinylbenzene and styrene (or any other vinyl monomer and/or divinyl crosslinking agent) in the presence of porogen (or diluent) [16]. Polymeric adsorbents can provide VOC capture efficiencies equivalent to conventional activated carbons and can capture a wide range of VOCs. Furthermore, the superior crush strength and spherical shape of polymeric adsorbents can reduce abrasion and extend the lifetime of the adsorbents [3]. Most importantly, the physical and chemical properties of polymeric

* Corresponding author. Tel.: +82 63 270 2312; fax: +82 63 270 2306.
E-mail address: yosklear@jbnu.ac.kr (Y.-S. Lee).

0304-3894/$ – see front matter © 2011 Elsevier B.V. All rights reserved.
doi:10.1016/j.jhazmat.2011.12.045

adsorbents can be adjusted by tailoring the monomers, crosslinkers, and diluents used to synthesize them.

Most studies regarding VOC recovery using microwaves have focused on polar VOCs because of their better absorption of microwave energy than nonpolar VOCs [17]. However, styrene–divinylbenzene polymeric adsorbents as well as nonpolar VOCs such as benzene are transparent to microwaves, and thus neither the adsorbents nor the nonpolar adsorbates are heated by microwaves. Some researchers have claimed that water should be supplied to overcome this problem [2,18], because of the excellent microwave absorption capacity of water, which could facilitate the indirect heating of the adsorbents [12]. We found that desorption of benzene from polymer adsorbents with hydroxyl groups was significantly facilitated by the presence of water vapor [19]. We synthesized these polymer adsorbents via hydrolysis of polymers beads with vinyl acetate units. However, the synthetic procedure was rather complicated due to inefficient alkaline hydrolysis and the low reactivity of the vinyl acetate monomers in the copolymerization reaction with divinylbenzene. Furthermore, hydroxyl groups may not be hydrophilic enough to efficiently capture water vapor.

In the study we report here, we prepared crosslinked 4-vinylpyridine–divinylbenzene copolymers followed by quaternization of the 4-vinylpyridyl units with iodomethane and post-crosslinking with ferric chloride. The effects of the hydrophilic methylpyridinium unit content on the benzene adsorption and desorption properties of the resulting polymer beads were studied under both dry and humid conditions.

2. Experimental

2.1. Materials

4-Vinylpyridine (4VP, 95% grade) was purchased from Aldrich. Divinylbenzene (DVB 55% grade) and poly(vinyl alcohol) were purchased from Nippon Steel Co. Ltd and OCI (South Korea), respectively. 2,2′-Azobisisobutyronitrile (AIBN), toluene, tricalcium phosphate (98–103%), and 1,2-dichloroethane were purchased from Daejung. Anhydrous ferric chloride ($FeCl_3$) was purchased from KANTO chemical. Polypropylene glycol (Mw 2000) was purchased from YAKURI Pure Chemical. Polymer beads, Optipore V503, were purchased from Dow Chemical Co. The water used in the present work was distilled and used without pH adjustment. All the chemicals were used as received.

2.2. Preparation of polymer beads

The macroporous polymer beads were prepared by suspension polymerization [20] using a 1.0 L four-necked separable round-bottomed flask fitted with a mechanical stirrer, a reflux condenser, and a thermometer. At room temperature, the flask was charged with the aqueous phase consisting of 270 mL water, 0.48 g poly(vinyl alcohol), 0.96 g tricalcium phosphate, and 0.8 mL methylene blue. The organic phase, a mixture of 4VP, DVB, diluents, and initiator (1.5 wt% to the monomers), was added to the aqueous phase. Polymerization was performed under stirring at 80 °C for about 15 h. The compositions of co-monomers are shown in Table 1. The prepared polymer beads were collected, washed with distilled water and acetone, and then dried. The polymer beads were pre-swollen in methylene chloride and extracted with the same solvent in Soxhlet apparatus for 15 h, then washed successively with pure solvent and solvent mixtures with gradually increasing solubility parameters [21], i.e., acetone, acetone/methanol, methanol, methanol/water, and finally distilled water. Afterwards, the beads were dried in air for 24 h, and then in oven at 60 °C. Polymer beads with diameters in the range of 0.3–1.0 mm were selected for further studies. The resulting polymer beads are abbreviated as D-4VP-0, D-4VP-10, D-4VP-20, and D-4VP-30, where the number after the second hyphen indicates the vol% of 4VP in each feed.

Table 1
Co-monomer compositions used for suspension polymerization.[a]

Monomer	D-4VP-0	D-4VP-10	D-4VP-20	D-4VP-30
DVB (ml)	40	36	32	28
4VP (ml)	0	4	8	12

[a] The ratio of the organic phase to the aqueous phase was 1:2.25 (v/v); the organic phase consisted of comonomers (DVB/4VP) and diluents (toluene and PPG 2000 in a 15:1 ratio in volume) in a 1:2 ratio (v/v)

2.3. Chemical modification of the as-prepared polymer beads

The polymer beads (12 g) were soaked in 100 mL acetone for 3 h, followed by addition of a large excess of iodomethane. The resulting mixture was kept at room temperature with occasional stirring for about 40 h [22]. Finally, the polymer beads were separated, washed with acetone and distilled water, then dried at 50 °C. The chemically modified polymer beads prepared from D-4VP-10, D-4VP-20, and D-4VP-30 are referred to as D-4VP-10M, D-4VP-20M, and D-4VP-30M, respectively.

2.4. Post-crosslinking of the polymer beads containing methyl pyridinium groups

The post-crosslinking reaction was carried out as described in the literature [23]. First, the starting polymer beads were fully swollen in 1,2-dichloroethane in a 1.0 L four-necked separable round-bottomed flask for 3 h. Under mild mechanical stirring, anhydrous ferric chloride (40 wt% of the starting polymer beads) was added slowly. After stirring for 1 h to achieve complete dispersion, the mixture was heated to 80 °C for 8 h. Finally, the polymer beads were washed with acetone, acetone/0.1 M HCl (1:1, v/v), and water, and then dried in an oven at 60 °C for at least 48 h before use. The post-crosslinked polymer beads made from the polymers of D-4VP-0, D-4VP-10M, D-4VP-20M, and D-4VP-30M are referred to as D-4VP-0C, D-4VP-10MC, D-4VP-20MC, and D-4VP-30MC, respectively.

2.5. Characterization

Infrared spectra were obtained on a FT-IR spectrometer (JASCO, 4100E). The surface morphologies of the polymer beads were determined using a scanning electron microscope (JEOL FE-SEM-5900) at 20 kV after coating the specimens with platinum. Specific surface areas and pore sizes of the adsorbents were calculated by the Brunauer, Emmet, and Teller (BET) treatment [24] and Barret, Joyner, and Halenda (BJH) [25] methods, respectively, via nitrogen adsorption and desorption on an ASAP 2010M instrument at 77 K. Before the BET surface area measurement, the adsorbents were degassed at 110 °C for 4 h.

2.6. Adsorption–desorption measurements

The VOC adsorption–desorption characteristics of the post-crosslinked polymer beads were investigated under dynamic conditions using a homemade apparatus. Polymer beads were dried in a vacuum oven at 60 °C overnight prior to each measurement. For comparison, commercial polymeric adsorbent Optipore V503 was selected as a reference, and its adsorption–desorption properties were investigated under the same conditions as used for the polymeric adsorbents synthesized in our laboratory. Several important

Table 2
Textural parameters of the polymer beads.

Sample	S_{BET}[a] ($m^2\ g^{-1}$)	V_t[b] ($ml\ g^{-1}$)	V_{mic}[c] ($ml\ g^{-1}$)	S_{ext}[d] ($m^2\ g^{-1}$)	S_{mic}[e] ($m^2\ g^{-1}$)	D_p[f] (Å)
D-4VP-0 C	754	1.57	0.11	493	261	134
D-4VP-10MC	572	1.41	0.09	367	205	161
D-4VP-20MC	289	1.13	0.01	256	33.5	211
D-4VP-30MC	176	0.81	–	170	6.28	225
Optipore V503	1,100	0.94	–	–	–	34

[a] Specific surface area (BET).
[b] Total pore volume.
[c] Microporous pore volume.
[d] External surface area.
[e] Specific microporous surface area.
[f] Average pore size.

textural parameters are summarized in Table 2 according to the product catalog provided by the Dow Chemical Company. The gas flow line for air supply was divided into two branches: one for pure air and the other for benzene vapor coming out through a benzene-bubbling apparatus in an oven at 20 °C. To determine the effects of humidity on adsorption and desorption, air was passed through a tube filled with calcium chloride (to remove moisture from the air) or a water-bubbling apparatus (to humidify the air). A mixture of benzene vapor and air was passed through a quartz tube (1 cm inner diameter × 13 cm length) containing polymer beads (tube length packed with polymer beads: 4 cm) at a flow rate of 110 mL/min. The concentration of benzene vapor in the inlet was fixed to be 1000 ppm using mass flow controllers. Both ends of the sample (quartz) tube filled with polymer adsorbents were sealed with glass fibers. Glass joints were securely sealed using Teflon tapes. Adsorption of benzene vapor by polymer beads was allowed to continue until a breakthrough point was attained, where the concentration of benzene in the outlet was approximately 5% of that in the inlet. For desorption, the gas flow (a mixture of benzene and air) was switched back to the pure air flow. The direction of carrier gas was changed in order to improve desorption efficiency, and then the polymer beads were irradiated with 600 W microwaves for 30 min after stabilization of the system with microwave irradiation for 10 min in the absence of the sample tubes. The flow rate for desorption was fixed at 100 mL/min. The concentration of benzene in the exit gas stream was monitored by a photoionization detector (PID). The amounts of benzene adsorbed and desorbed were calculated by integrating the outlet benzene concentration-time curves.

3. Results and discussion

3.1. Synthesis of polymer adsorbents

FT-IR spectra of the initial polymer beads are presented in Fig. 1. The spectra exhibit absorption peaks located at 1599, 1487, 1414, and 994 cm^{-1}, which are attributable to the characteristic vibrations of the pyridiyl moieties [26,27]. The next strong peaks at 1069 and 820 cm^{-1} are also assigned to the in-plane and out-of-plane bending vibrations of the pyridiyl units, respectively [27,28]. The intensities of these peaks increased significantly as the content of 4VP in the feed increased. This result suggests that 4VP was successfully copolymerized along with DVB and incorporated into the polymer beads.

FT-IR spectra of the modified polymer beads with iodomethane are shown in Fig. 2. The absorption peak at 1599 cm^{-1} was significantly reduced, but the peak at 1414 cm^{-1}, clearly present in Fig. 1, almost disappeared. Instead, a new peak at 1640 cm^{-1}, a characteristic peak for a quaternized pyridiyl group, is apparent. This result indicates that the pyridiyl groups in the polymer beads were almost completely quaternized [27,28].

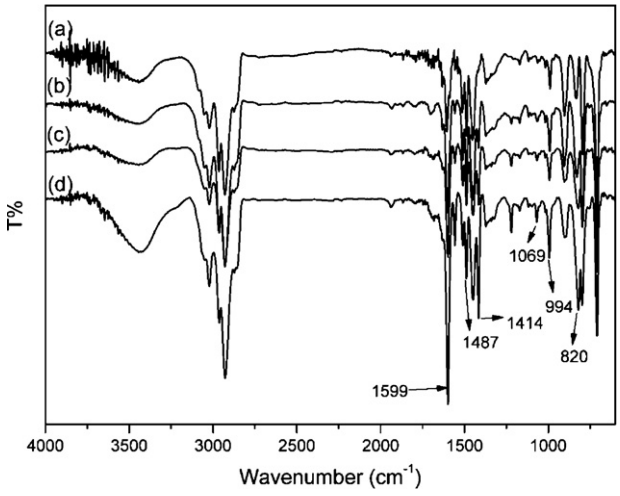

Fig. 1. FT-IR spectra of polymer beads: (a) D-4VP-0, (b) D-4VP-10, (c) D-4VP-20, and (d) D-4VP-30.

The post-crosslinked products were also characterized by FT-IR, and their spectra are shown in Fig. 3. Post-crosslinking is evidenced by the disappearance of the characteristic peaks of unreacted vinyl groups of the DVB units located at 990 and 1630 cm^{-1} [23], but the peak at 1630 cm^{-1} overlaps with the methyl pyridinium peak at 1640 cm^{-1}. The peak at 990 cm^{-1} almost completely disappeared for D-4VP-10M, and was significantly reduced for D-4VP-20M and D-4VP-30M, indicating that post-crosslinking was fairly efficient in the presence of excess $FeCl_3$ catalyst.

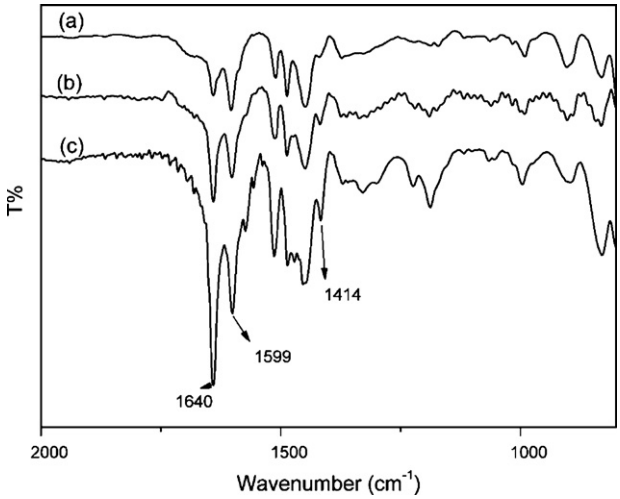

Fig. 2. FT-IR spectra of the polymer beads modified with iodomethane: (a) D-4VP-10 M, (b) D-4VP-20 M, and (c) D-4VP-30 M.

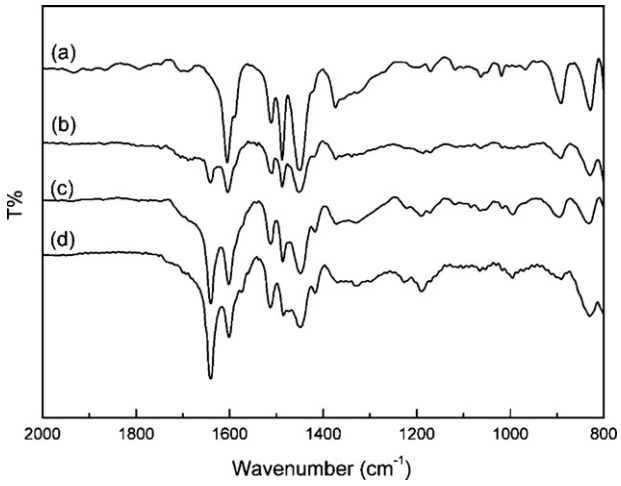

Fig. 3. FT-IR spectra of post-crosslinked polymer beads: (a) D-4VP-0 C, (b) D-4VP-10MC, (c) D-4VP-20 MC, and (d) D-4VP-30MC.

3.2. Determination of physical structure

Nitrogen adsorption and desorption isotherms of post-crosslinked polymer beads are shown in Fig. 4. The obtained isotherms were type IV isotherms, indicating the presence of medium to large pores in the polymers [29,30]. The adsorption and desorption branches coincided at lower relative pressures, indicating reversible nitrogen adsorption. After formation of nitrogen multilayers, capillary condensation occurs as all the pores are progressively filled. It is known that during adsorption, condensation starts from the narrowest pores while evaporation during desorption begins from the largest pores. This difference is the major cause of the hysteresis between adsorption and desorption isotherms observed at the higher relative pressures [31]. The four different polymer beads showed very similar hysteresis in their adsorption–desorption isotherms, indicating that their pore structures were similar.

Table 2 lists some important characteristics of the polymer beads. The surface areas of the polymer beads were calculated from the above nitrogen sorption isotherms using the (BET) [21]. The pore volumes and average pore sizes were determined from the adsorption branches of the isotherms by the (BJH) method [25]. Both the specific surface area and pore volume decreased markedly as the content of 4VP in the polymer beads increased,

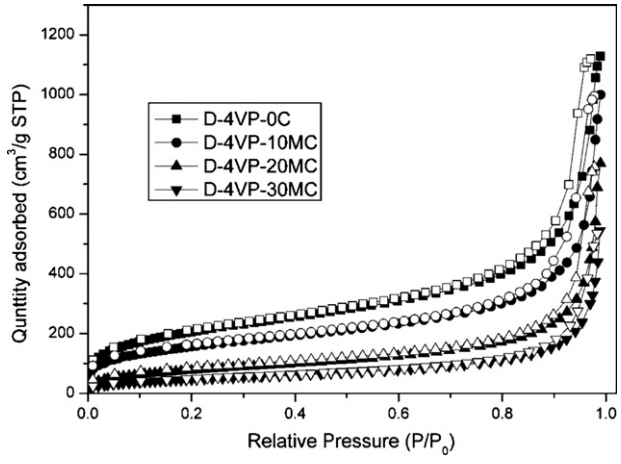

Fig. 4. Nitrogen adsorption–desorption isotherms for the post-crosslinked polymer beads: closed and open symbols correspond to adsorption and desorption branches, respectively.

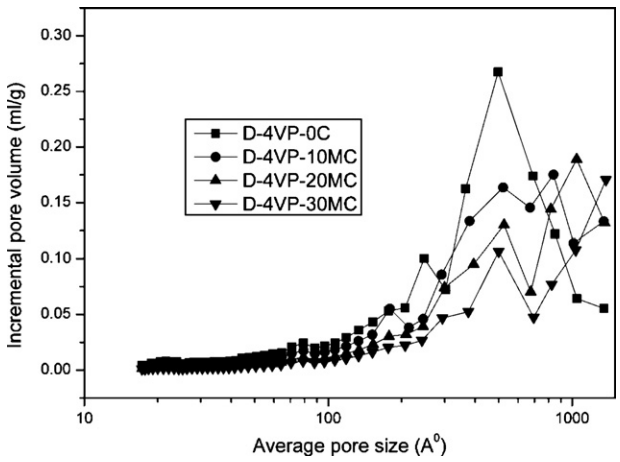

Fig. 5. Pore size distributions of the post-crosslinked polymer beads as determined by the BJH method using the nitrogen adsorption isotherm data.

while the average pore size increased continuously. We attribute this change mainly to a decrease in the crosslinking density as the content of DVB increased. Furthermore, the solubility parameters of toluene, styrene–DVB copolymer, and poly(4VP) are 18.3, 18 [28], and 21.5 $MPa^{1/2}$ [32], respectively, indicating that toluene is a good solvent for the styrene–DVB copolymer, but a poor solvent for poly(4VP). This can also at least partially explain the characteristics of the pores; increasing the content of poor solvent in pore-forming agents results in a decrease in the surface area and pore volume but an increase in the pore size [16].

The pore size distributions of the polymer beads were estimated by the BJH method, and the results are shown in Fig. 5. Most pores in D-4VP-0 C had diameters in the range of 300–1400 Å with a maximum of approximately 500 Å. As the 4VP content increased, the pore size distributions of the other beads shifted to the larger size region. The maximum peaks in the pore size distribution curves of D-4VP-10MC and D-4VP-20MC were located at approximately 800 and 1000 Å, respectively. The maximum peak in the distribution curve of D-4VP-30MC was beyond our measurement range. These results indicate that the polymer beads were essentially macroporous. This result can be explained in terms of the crosslinking density of the polymer beads and the solubility parameters of the diluents, as discussed above. As the content of 4VP increased, the solvating power of the diluents decreased, phase separation occurred before the gel point, and consequently, the polymer particles became crosslinked to form nuclei that then agglomerated. Agglomeration of the nuclei resulted in the formation of microspheres, which further agglomerated into irregular particles within a polymer structure [21]. Mesopores (20–500 Å in diameter) and macropores (>500 Å in diameter) have been shown to form between agglomerates of microspheres [33]. Therefore, the higher specific surface area of D-4VP-0C compared to the other adsorbents is due not only to its larger pore volume but also its smaller pore size.

3.3. Dynamic adsorption–desorption

In this study, we measured adsorption and desorption under dynamic conditions rather than static conditions, because the former more closely reflects practical conditions. We evaluated the dynamic adsorption–desorption performances of the polymer beads by monitoring the adsorbate–desorbate concentrations in the outlet over time [31]. We defined breakthrough adsorption capacity to be the amount of benzene adsorbed until the outlet concentration of the adsorbate reached 5% of the inlet adsorbate concentration [34]. In this study, benzene was selected as a model

Table 3
Summary of adsorption–desorption characteristics of benzene on different polymeric adsorbents.

Adsorbent	Breakthrough time (min)	Adsorption capacity (mg/g)	Desorption capacity (mg/g)	Desorption efficiency (%)
D-4VP-0 C[a]	42	21	9.9	47
D-4VP-0 C[b]	42	21	9.9	47
D-4VP-10MC[a]	36	16	8.5	53
D-4VP-10MC[b]	24	10	6.6	66
D-4VP-20MC[a]	33	14	7.4	53
D-4VP-20MC[b]	16	7.1	6.2	87
D-4VP-30MC[a]	18	6.9	–	–
D-4VP-30MC[b]	8.0	3.1	–	–
Optipore V503[a]	186	64	6.6	10
Optipore V503[b]	144	52	19	37

[a] In dry air.
[b] In humidified air with a relative humidity of about 70%.

nonpolar VOC because it is widely eluted by industries and is a serious environmental pollutant. The experimental data for the polymer beads are summarized in Table 3.

The breakthrough adsorption capacity of D-4VP-0 C was the highest, and decreased as the 4VP content increased under both dry and humidified conditions. This result is consistent with the hydrophobicity and crosslinking density (consequently pore volume and specific surface area) of the polymer beads, which are closely related to the contact efficiency and affinity of the polymer adsorbent and flow stream. First, adsorption of benzene on polymer beads will be less efficient as the hydrophilicity of the polymer beads increases, which is achieved simply by increasing the content of methylpyridinium unit. The affinity of the polymer beads for benzene is also expected to decrease as their hydrophilicity increases. Second, the adsorption capacity of polymer beads will increase as the pore volume and specific surface area of the beads increase; adsorption capacity decreased as the content of methylpyridinium unit increased, as expected. The microporosity of the polymer beads should be also considered. It is known that the adsorption occurs through diffusion into macropores before adsorbate fixation in accessible pores such as mesopore and/or micropore. Thus the adsorption capacity of an adsorbent is largely dependent on its microporosity [35,36]. The microporosity of our polymer beads decreased as the content of methylpyridinium unit increased, which is in good agreement with the trend in adsorption capacity. The breakthrough time and adsorption capacity of Optipore V503 were much longer and higher, respectively, than those of our polymer beads, probably due to the significantly higher specific surface area and smaller pore sizes of Optipore V503.

The adsorption of VOCs from a wet fluid is a complex process [37]. However, moisture in the fluid had a clear effect on the polymer adsorbents, as shown in Table 3. The breakthrough times of D-4VP-0 C under dry and humid air conditions were the same, but those of the other polymer adsorbents with hydrophilic methylpyridinium groups were shorter under humid conditions than dry conditions. Furthermore, the breakthrough time became significantly shorter under humid conditions as the content of hydrophilic units increased. In particular, D-4VP-30MC had the shortest breakthrough time (only about 56% of the breakthrough time under dry conditions). This result can be explained as follows: as the affinity between hydrophilic groups in the polymer adsorbents and moisture in the air increases, more adsorption sites will be occupied by water vapor, less adsorption sites will be available for benzene vapor, and consequently less benzene vapor will be adsorbed, leading to a shorter breakthrough time. The breakthrough adsorption capacity of Optipore V503 under humid conditions was slightly lower than that under dry conditions, suggesting that it may be slightly polar.

The relative humidity at the outlet of the adsorption–desorption tube packed with the polymer adsorbents were measured as a function of the flowing time of humidified air, and the results are presented in Fig. 6. The initial relative humidity at the outlet was not zero due to the limitations of the simple hygrometer used for measurement. In the case of D-4VP-0 C, the relative humidity at the outlet increased rapidly to the same level as that at the inlet within 2 min, indicating that the most hydrophobic adsorbent did not adsorb the moisture efficiently under these conditions and that water vapor in the air immediately passed through the adsorption tube. In the case of D-4VP-10 C, the relative humidity at the outlet increased slowly and was close to that at the inlet within the breakthrough time (24 min, see Table 3). In contrast, in the case

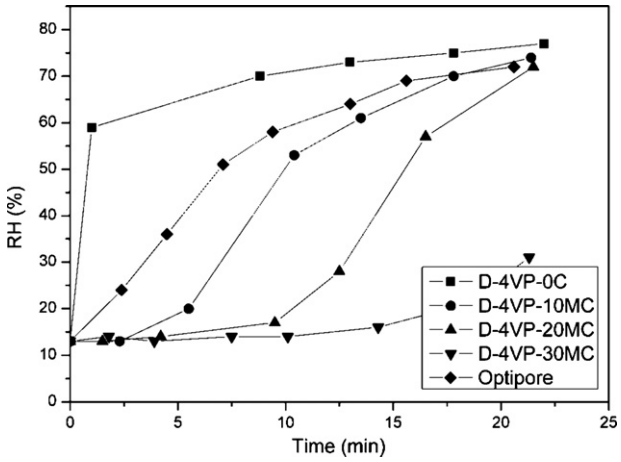

Fig. 6. Relative humidity at the outlet of the sample tube packed with polymer adsorbents as a function of the flowing time of humidified air with a relative humidity of 80%.

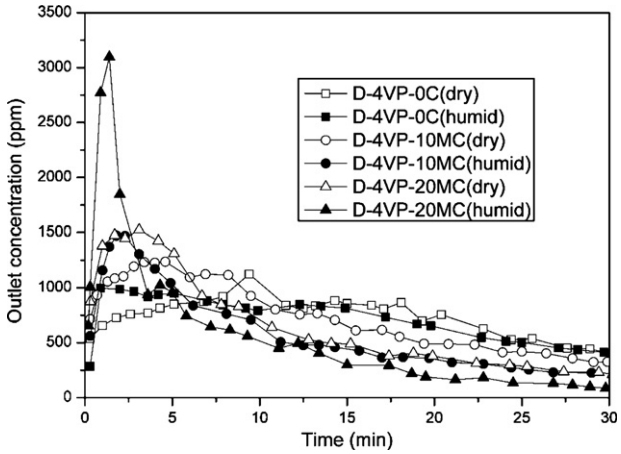

Fig. 7. Desorption of benzene from various polymer adsorbents under dry and humid air conditions upon irradiation with 600 W microwaves.

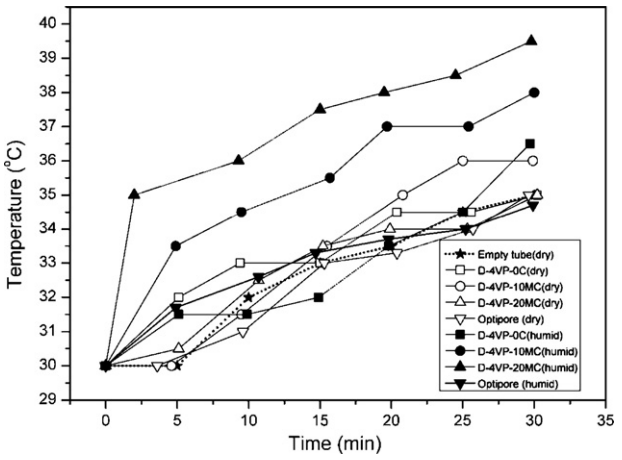

Fig. 8. Temperatures of the quartz tubes packed with polymer adsorbents as a function of irradiation time with 600 W microwaves for 30 min.

of D-4VP-20 C, the relative humidity at the outlet increased much more slowly and was much lower than that at the inlet within the breakthrough time (16 min), while for D-4VP-30 C, the relative humidity at the outlet essentially did not increase and remained largely unchanged within the breakthrough time (8 min). This result indicates that as the polymer hydrophilicity increased, the amount of moisture adsorbed by the polymer adsorbents increased, and consequently the breakthrough time for adsorption of water vapor increased. On the other hand, the variation curve of relative humidity for Optipore V503 is located between those of D-4VP-0 C and D-4VP-10MC. Based on this result along with the humidity-dependent breakthrough adsorption capacity, the hydrophilicity of Optipore V503 seems to be in between that of D-4VP-0 C and D-4VP-10MC.

The desorption of benzene from the polymer adsorbents under dry and humid air conditions upon irradiation with 600 W microwaves for 30 min is shown in Fig. 7. D-4VP-30MC was excluded from this experiment because of its low adsorption capacity compared with the other samples. The desorption efficiency of D-4VP-0 C was 48% regardless of whether water vapor was supplied or not. The desorption efficiencies of D-4VP-20MC were 52 and 87% under dry and humid conditions, respectively, and the desorption efficiencies of D-4VP-10MC under the two different conditions were located in between those of D-4VP-0 C and D-4VP-20MC. The maximum concentration of desorbed benzene vapor in the outlet gas stream increased with an increasing content of methyl pyridinium unit. In other words, more polar polymer adsorbents concentrate benzene more effectively during shorter microwave-irradiation times under humid conditions than less polar polymer adsorbents. For example, in the case of D-4VP-20MC, the maximum concentration of benzene vapor in the outlet under humid conditions was up to three-fold the concentration of benzene in the inlet. Desorption of benzene from Optipore V503 was also investigated, but these data were not included in Fig. 7, because the desorption efficiencies of benzene from Optipore V503 under both dry and humid conditions were significantly lower than those of the other samples. The much less efficient desorption of benzene from Optipore V503 than observed for our polymers might be due to the much smaller pore sizes of Optipore V503 than our polymers, which could make the desorption of adsorbed benzene more difficult and decrease the effectiveness of microwave heating because of the lower hydrophilicity of the pores. In addition, the higher adsorption capacity of Optipore V503 compared with our adsorbents could also be a contributing factor to the less efficient desorption of benzene.

Under humidified conditions, the microwave-assisted desorption of benzene vapor from the polymer absorbents clearly increased as the content of hydrophilic unit in the polymer increased. These experimental results can be explained as follows. First, ordinary polymers are transparent or semitransparent to microwaves, and are therefore not efficiently heated by microwaves [2]. In contrast, polymers containing hydrophilic units can be heated by microwave-absorbing hydrophilic units and/or adsorbed moisture. Second, nonpolar benzene is probably more strongly bonded to the surface of less polar (hydrophobic) adsorbents such as D-4VP-0 C, and is therefore more difficult to be desorbed from the adsorbents. Third, the flush effect, i.e., overshooting of benzene vapor by water vapor, also contributes to the desorption process [18]. In other words, immediately after microwave-irradiation has started, adsorbed water on the polymer beads is heated and desorbed, and then a part of the desorbed water moves with carrier gas (air) to another adsorption zone where benzene is adsorbed. At this point, the water molecule will competitively adsorb on the adsorption zone and the benzene molecule will be desorbed, leading to more concentrated benzene vapor in the outlet.

3.4. Measurement of the temperature of the adsorption–desorption tube

As described above, we attributed the microwave-assisted desorption of benzene vapor from the polymer beads mainly to a thermal effect whereby adsorbed water molecules on the polymer beads absorbed microwaves and converted them to heat. To confirm this hypothesis, we monitored the temperature of each adsorption–desorption tube during irradiation with 600 W microwaves, and the results are presented in Fig. 8. Direct temperature measurement of the adsorbent tube during microwave heating without disturbing the microwave field was difficult. Therefore, we measured the temperatures of the quartz tubes packed with polymer adsorbents as follows. After a pre-determined time interval of continuous microwave irradiation, the microwave power was switched off and the temperature of tube was measured as quickly as possible using an infrared thermometer, while gas flow through the adsorption tube was maintained. Our experimental results show that the temperatures of the tubes increased slowly up to 35–36 °C with irradiation time even under dry conditions, but increased more rapidly up to 36–40 °C, under humid air conditions. It is interesting to note that benzene was desorbed from the polymeric adsorbents at the relatively low temperatures. This result can be attributed to some reasons. First, the temperatures measured by the infrared thermometer were the temperatures of the tube's external surface which may be lower than the actual temperatures of polymer beads. Second, the relatively large pore sizes of the polymer beads might cause the easy desorption. Third, the direction of carrier gas flow was changed, and the adsorbed benzene vapor might be concentrated at a region near to the tube outlet, leading to the easy desorption.

Under humid air conditions, the effect of the content of hydrophilic unit on the temperature increase became more significant. This observation supports our hypothesis that microwave heating of the polymer beads is due mainly to the presence of adsorbed water. The temperature increase of the quartz tube packed with Optipore V503 was very similar to that of the tube packed with D-4VP-0 C under humid conditions, indicating that microwave heating of Optipore V503 is an ineffective process. The slight increase in the temperature observed under dry air conditions may result from a small amount of remaining moisture in the polymer beads [18] and the raised temperature within the microwave oven. The temperature change observed in the empty tube confirmed the latter explanation.

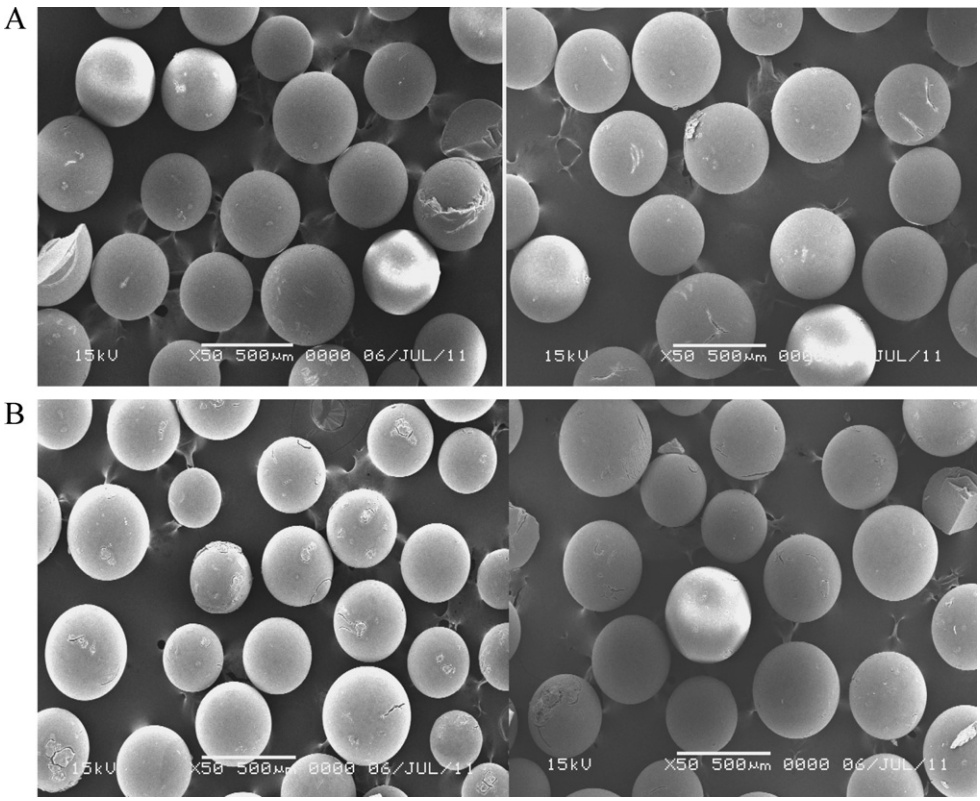

Fig. 9. Scanning electron micrographs of polymer beads before (left) and after (right) the adsorption–desorption process: (A) D-4VP-10MC and (B) D-4VP-20MC.

3.5. Scanning electron micrographs of polymer adsorbents

Scanning electron micrographs of D-4VP-10MC and D-4VP-20MC before and after the adsorption–desorption process are presented in Fig. 9. Most polymer beads were approximately spherical and their surfaces were smooth. The shape and surface morphology of the regenerated adsorbents remained relatively unchanged, indicating that the adsorption–desorption process does not damage the polymer adsorbents. Some minor scratches may occur during loading of the polymer beads into the packing tube, but this is unlikely to affect the absorption–desorption characteristics of the polymer beads. Thus, these polymer beads can be repeatedly used as adsorbents in microwave-assisted recovery systems.

4. Conclusions

In the present study, we successfully synthesized macroporous polymer beads with and without hydrophilic methylpyridium groups via suspension polymerization of divinylbenzene and 4VP, quaternization with iodomethylation, and post-crosslinking with ferric chloride. As the 4VP content in the feed increased, the BET surface area of the resulting polymer beads decreased, but their pore size increased due to a decrease in crosslinking density and the lower solubility of poly (4VP) in toluene. As the content of hydrophilic unit in the polymer adsorbents increased, the breakthrough time for benzene vapor decreased significantly along with the corresponding breakthrough adsorption capacity under humidified air conditions. As the content of hydrophilic unit in the polymer adsorbents increased from 0 to 20%, their desorption efficiency increased significantly from 48 to 87% under humidified air conditions. We attributed the enhanced desorption efficiency mainly to more adsorbed moisture that indirectly heated the polymer adsorbents to higher temperatures upon microwave irradiation. Even though there is still scope for improvement, our initial results are encouraging. We are currently determining the effects of the BET surface areas and pore sizes of the polymer beads on their adsorption–desorption efficiencies, and anticipate reporting our findings in the near future.

References

[1] F.I. Khan, A.K. Ghoshal, Removal of volatile organic compounds from polluted air, J. Loss Prevent Proc. 13 (2000) 527–545.
[2] P. Di, D.P.Y. Chang, Microwave regeneration of volatile organic compound (VOC) adsorbents, in: Air & Waste Management Association. 89th Annual Meeting and Exhibition, Nashville, 1996.
[3] S.H. Opperman, R.C. Brown, VOC emission control with polymeric adsorbents and microwave desorption, Pollut. Eng. 31 (1999) 58–60.
[4] J. Reuß, D. Bathen, H. Schmidt-Traub, Desorption by microwaves: mechanisms of multicomponent mixtures, Chem. Eng. Technol. 25 (2002) 381–384.
[5] Z. Hashisho, M. Rood, L. Botich, Microwave-swing adsorption to capture and recover vapors from air streams with activated carbon fiber cloth, Environ. Sci. Technol. 39 (2005) 6851–6859.
[6] M.D. Turner, R.L. Laurence, W.C. Conner, K.S. Yngvesson, Microwave radiation's influence on sorption and competitive sorption in zeolites, AlChE J. 46 (2000) 758–768.
[7] R. Cherba'nski, M. Komorowska-Durka, G.D. Stefanidis, A.I. Stankiewicz, Microwave swing regeneration vs temperature swing regeneration-comparison of desorption kinetics, Ind. Eng. Chem. Res. 50 (2011) 8632–8644.
[8] R. Cherba'nski, E. Molga, Intensification of desorption processes by use of microwaves—an overview of possible applications and industrial perspectives, Chem. Eng. Process 48 (2009) 48–58.
[9] W.G. Shim, J.W. Lee, H. Moon, Adsorption equilibrium and column dynamics of VOCs on mcm-48 depending on pelletizing pressure, Microporous Mesoporous Mater. 88 (2006) 112–125.
[10] C. Parmele, T. Kovalcson, Adsorption: Carbon, in: H.J. Rafson (Ed.), Odor and VOC Control Handbook, vol. 8, McGraw-Hill, New York, 1998, pp. 66–93.
[11] J.H. Yun, D.K. Choi, S.H. Kim, Adsorption of organic solvent vapors on hydrophobic y-type zeolite, AlChE J. 44 (1998) 1344–1350.
[12] K.J. Kim, Y.H. Kim, W.J. Jeong, N.C. Park, S.W. Jeong, H.G. Ahn, S.Q.Y.T. Dongyuan Zhao, Y. Chengzhong, Adsorption–desorption characteristics of volatile organic compounds over various zeolites and their regeneration by microwave irradiation, Stud. Surf. Sci. Catal. 165 (2007) 223–226.

[13] Q. Hu, J. Li, S. Qiao, Z. Hao, H. Tian, C. Ma, C. He, Synthesis and hydrophobic adsorption properties of microporous/mesoporous hybrid materials, J. Hazard. Mater. 164 (2009) 1205–1212.
[14] H. Zaitan, D. Bianchi, O. Achak, T. Chafik, A comparative study of the adsorption and desorption of o-xylene onto bentonite clay and alumina, J. Hazard. Mater. 153 (2008) 852–859.
[15] V. Davankov, M. Tsyurupa, A.D. Vadim, P.T. Maria, Sorption of gases and organic vapors Comprehensive Analytical Chemistry, vol. 56, Elsevier, 2011, pp. 370–409 (Chapter 10).
[16] S. Kara, O. Okay, O. Pekcan, In situ photon transmission technique for monitoring phase separation in real time during gelation, Polym. Bull. 45 (2000) 281–285.
[17] C.O. Ania, J.A. Menéndez, J.B. Parra, J.J. Pis, Microwave-induced regeneration of activated carbons polluted with phenol. A comparison with conventional thermal regeneration, Carbon 42 (2004) 1383–1387.
[18] S.I. Kim, T. Aida, H. Niiyama, Binary adsorption of very low concentration ethylene and water vapor on mordenites and desorption by microwave heating, Sep. Purif. Technol. 45 (2005) 174–182.
[19] M.L. Hwang, Y.S. Lee, T.G. Kim, G.S. Yang, T.S. Park, Y.S. Lee, Synthesis of hydroxylated macroporous polymer beads for microwave-assisted desorption of nonpolar volatile organic compounds, Bull. Korean Chem. Soc. 31 (2010) 1–4.
[20] X. Zeng, T. Yu, P. Wang, R. Yuan, Q. Wen, Y. Fan, C. Wang, R. Shi, Preparation and characterization of polar polymeric adsorbents with high surface area for the removal of phenol from water, J. Hazard. Mater. 177 (2010) 773–780.
[21] A.W. Trochimczuk, S. Aoki, K. Yamabe, A. Jyo, Synthesis of porous divinylbiphenyl copolymers and their sorptive properties towards phenol and its derivatives, Eur. Polym. J. 38 (2002) 1175–1181.
[22] M. Giammatteo, L. Tauro, A.A. D'archivio, L. Galantini, A. Panatta, E. Tettamanti, K. Jerabek, B. Corain, Cross-linked poly-4-vinylpyridines as useful supports in metal catalysis: micro- and nanometer scale morphology, J. Mol. Catal. A: Chem. 268 (2007) 176–184.
[23] X. Zeng, Y. Fan, G. Wu, C. Wang, R. Shi, Enhanced adsorption of phenol from water by a novel polar post-crosslinked polymeric adsorbent, J. Hazard. Mater. 169 (2009) 1022–1028.
[24] S. Brunauer, P.H. Emmett, E. Teller, Adsorption of gases in multimolecular layers, J. Am. Chem. Soc. 60 (1938) 309–319.
[25] E.P. Barrett, L.G. Joyner, P.P. Halenda, The determination of pore volume and area distributions in porous substances I. Computations from nitrogen isotherms, J. Am. Chem. Soc. 73 (1951) 373–380.
[26] N. Fontanals, R.M. Marcé, M. Galià, F. Borrull, Preparation and characterization of highly polar polymeric sorbents from styrene–divinylbenzene and vinylpyridine–divinylbenzene for the solid-phase extraction of polar organic pollutants, J. Polym. Sci. Part A: Polym. Chem. 41 (2003) 1927–1933.
[27] G. Li, J. Shen, Y. Zhu, A study of pyridinium-type functional polymers iii: preparation and characterization of insoluble pyridinium-type polymers, J. Appl. Polym. Sci. 78 (2000) 668–675.
[28] D. Jermakowicz-Bartkowiak, B.N. Kolarz, Poly(4-vinylpyridine) resins towards perrhenate sorption and desorption, React. Funct. Polym. 71 (2011) 95–103.
[29] K.S.W. Sing, D.H. Everett, R.A.W. Haul, L. Moscou, R.A. Pierotti, J. Rouquerol, T. Siemieniewska, Reporting physisorption data for gas/solid systems with special reference to the determination of surface area and porosity pure, Appl. Chem. 57 (1985) 603–619.
[30] K. Sing, The use of nitrogen adsorption for the characterisation of porous materials, Colloids Surf. A 187–188 (2001) 3–9.
[31] T. Chafik, S. Harti, G. Cifredo, J.M. Gatica, H. Vidal, Easy extrusion of honeycomb-shaped monoliths using moroccan natural clays and investigation of their dynamic adsorptive behavior towards VOCs, J. Hazard. Mater. 170 (2009) 87–95.
[32] K.S. Dennis, Inventor the Dow Chemical Company, Assignee, gelled organic liquid and method for making (1989).
[33] C.M. Cheng, F.J. Micale, J.W. Vanderhoff, M.S. El-Aasser, Pore structural studies of monodisperse porous polymer particles, J. Colloid Interface Sci. 150 (1992) 549–558.
[34] G. Marb, A.B. Fuertes, Co-adsorption of n-butane/water vapour mixtures on activated carbon fibre-based monoliths, Carbon 42 (2004) 71–81.
[35] A.B. Fuertes, G. Marb, D.M. Nevskaia, Adsorption of volatile organic compounds by means of activated carbon fibre-based monoliths, Carbon 41 (2003) 87–96.
[36] D.M. Ruthven, Past progress and future challenges in adsorption research, Ind. Eng. Chem. Res. 39 (2000) 2127–2131.
[37] F. Cosnier, A. Celzard, G. Furdin, D. Bégin, J.F. Marêché, Influence of water on the dynamic adsorption of chlorinated VOCs on active carbon: relative humidity of the gas phase versus pre-adsorbed water, Adsorpt. Sci. Technol. 24 (2006) 215–228.